PRAMANA — journal of physics

Vol. 78, No. 3
March 2012
pp. 347–360

Nonlinear resonance in Duffing oscillator with fixed and integrative time-delayed feedbacks

V RAVICHANDRAN[1], V CHINNATHAMBI[1,*] and S RAJASEKAR[2]
[1]Department of Physics, Sri K.G.S. Arts College, Srivaikuntam 628 619, India
[2]School of Physics, Bharathidasan University, Thiruchirapalli 620 024, India
*Corresponding author. E-mail: v_chin2005@yahoo.com

MS received 29 June 2011; revised 24 September 2011; accepted 14 October 2011

Abstract. We study the nonlinear resonance, one of the fundamental phenomena in nonlinear oscillators, in a damped and periodically-driven Duffing oscillator with two types of time-delayed feedbacks, namely, fixed and integrative. Particularly, we analyse the effect of the time-delay parameter α and the strength γ of the time-delayed feedback. Applying the perturbation theory we obtain a nonlinear equation for the amplitude of the periodic response of the system. For a range of values of γ and α, the response amplitude is found to be higher than that of the system in the absence of delayed feedback. The response amplitude is periodic on the parameter α with period $2\pi/\omega$ where ω is the angular frequency of the external periodic force. We show the occurrence of multiple branches of the response amplitude curve with and without hysteresis.

Keywords. Duffing oscillator; nonlinear resonance; time-delayed feedback; hysteresis.

PACS Nos 05.45.Ac; 05.45.Pq; 05.45.Xt

1. Introduction

Time-delay is ubiquitous in many nonlinear dynamical systems because of finite switching speed of the amplifiers, finite reaction times, finite signal propagation time in biological networks, memory effects and so on [1–3]. When the response of a deterministic dynamical system at time t depends on its state at a shifted earlier time $t-\alpha$; $\alpha > 0$, then a time-delayed feedback can be introduced in the equation of motion of the system. In interaction coupled systems, the coupling can be time-delayed. The time-delayed feedback and coupling can be linear or nonlinear. The influence of fixed time-delayed feedback of the form $x(t-\tau)$, where x is a state variable, has been investigated in nonlinear systems. Several interesting phenomena, such as novel bifurcations [4,5], amplitude death [6], hyperchaos [7], strange nonchaotic attractor [8], stochastic dynamics [9–11], excitation regeneration [12], re-entrance phenomenon [13,14], patterns [15] and multiple vibrational resonance [16–18] were found. Linear time-delayed self-feedback can be

DOI: 10.1007/s12043-011-0244-7; ***e*Publication: 2 March 2012**

realized in many physical and biological systems. For example, the use of an optical reflection with the help of a semitransparent mirror of reflectivity L in a laser unit gives rise to such a time-delayed feedback of strength L [19,20]. In a cutting process, the presence of machine tool vibration due to some external disturbances gives rise to a cutting force that depends on a delayed value of the displacement [21].

Dynamical effects due to another type of time-delay, namely, integrative time-delay [22–27] has also been analysed in certain nonlinear systems. In the integrative time-delayed feedback, the feedback is integrated over a time interval α: $\int_{t-\alpha}^{t} f(x(t'))\mathrm{d}t'$. The feedback is not only time-delayed but also cumulative over a certain time interval α. This kind of time-delay was earlier introduced in the 'integrate-and-fire' models [22] and self-organized critically [24]. When the growth of the species depends on the concentration of nutrients over a certain interval of past time then one has to include this type of time-delayed feedback. Under certain conditions, the neuronal population discharge dynamics of both cortical and thalamic slices reduces to a model of integrate-and-fire neurons where each neuron can fire only one spike. When the membrane potential of a neuron reaches a threshold value the neuron fires a spike and cannot fire more spikes afterwards and this is represented by the integrative time-delayed coupling term [25]. In a two-coupled Landau–Stuart oscillators, the integrative time-delayed coupling is shown to induce an amplitude death (bifurcation from a periodic orbit to a stable equilibrium point) even when the interacting systems are identical over a wide region of parameter space [27]. Recently, multitime-delayed feedback on stochastic resonance has been analysed in a bistable system [28].

In recent years great interest has been focussed on exploiting nonlinear systems for detecting weak signals and for enhancing the output signal. It has been realized that in nonlinear systems, response to a weak input periodic signal can be enhanced by means of external noise and high-frequency second periodic force and the resulting phenomena are called stochastic resonance [29] and vibrational resonance [30] respectively. In this connection, it is noteworthy to mention that only local information is often used in the signal amplification in many physical and biological systems. Thus, it is important to explore the possibility of improving the response of a single system by means of feedback signals. Motivated by the above considerations, in the present work we consider the effect of both fixed time-delayed and integrative time-delayed feedbacks on the enhancement of response of a system. Particularly, we study the nonlinear resonance, one of the fundamental phenomena in periodically-driven nonlinear oscillators, where the response amplitude becomes maximum at a specific frequency of the input signal, in the damped and periodically-driven Duffing oscillator with the above two feedbacks.

The equation of motion of the Duffing oscillator of our interest is

$$\ddot{x} + d\dot{x} + \omega_0^2 x + \beta x^3 + \gamma F(x(t-\alpha)) = f\cos\omega t, \tag{1}$$

where $F(x(t-\alpha))$ is the time-delayed feedback. For the fixed and integrative time-delayed feedbacks, $F = x(t-\alpha)$ and $(1/\alpha)\int_{t-\alpha}^{t} x(t')\mathrm{d}t'$ respectively. For both types of feedbacks, by applying a perturbation theory, we obtain the equation of motion for the amplitude and phase of an assumed sinusoidally varying solution. The equilibrium points of this equation of motion represent the steady-state solution of the amplitude and phase of the periodic solution. We obtain decoupled equations for the response amplitude and phase. We fix the values of the parameters ω_0^2, d, β and f such that in the absence

of delayed feedback the frequency–response curve is multivalued and typical nonlinear resonance with hysteresis and jump phenomena occurs. We study the effect of time-delayed feedback parameters γ and α on resonance. For a range of fixed values of γ and α, the enhancement of response amplitude takes place when the frequency of the external periodic force is varied. Suppression of hysteresis occurs for a certain range of fixed values of γ and α. Both $\omega_{\max}$, the value of ω at which the response amplitude A becomes maximum, and $A_{\max}$, the maximum value of A, vary in a sinusoidal manner with the parameter α. $\gamma > 0$ and $\gamma < 0$ have inverse effect on the variation of $\omega_{\max}$ and $A_{\max}$. When α is varied the response amplitude curve is single-valued for a range of fixed values of ω. Multiple branches of response amplitude curve occurs for certain fixed values of ω. We have examples for response with and without hysteresis. Another interesting result is that the response amplitude profile is periodic on the parameter α with period $2\pi/\omega$. $\alpha_{\max}$, the value of α at which A is maximum, decreases with increase in the value of ω for both $\gamma < 0$ and $\gamma > 0$. We compare the theoretical predictions with numerical results. We found very good agreement between theoretical predictions and numerical results.

2. Effect of fixed time-delayed feedback

First, applying a perturbation theory to eq. (1) with the fixed time-delayed feedback, namely $F(x(t-\alpha)) = x(t-\alpha)$, we obtain a nonlinear equation for the amplitude A of a period-$T(=2\pi/\omega)$ solution and analyse the effect of time-delayed feedback on the amplitude A.

2.1 *Theoretical expression for response amplitude*

We assume the solution of (1) as

$$x(t) = a(t)\cos\omega t + b(t)\sin\omega t, \tag{2}$$

where $a(t)$ and $b(t)$ are slowly varying functions of time t. Substituting the solution (2) and

$$x^3 \approx \frac{3}{4}(a^2+b^2)(a\cos\omega t + b\sin\omega t), \tag{3}$$

in eq. (1), neglecting $\ddot{a}$, $\ddot{b}$, $\mathrm{d}\dot{a}$ and $\mathrm{d}\dot{b}$ as they are assumed to be small and then equating the coefficients of $\sin\omega t$ and $\cos\omega t$ separately to zero we obtain

$$\dot{a} = -\frac{b}{2\omega}\left[\omega^2 - \omega_0^2 - \frac{3}{4}\beta(a^2+b^2)\right] - \frac{\mathrm{d}a}{2} + \frac{\gamma}{2\omega}\left[a(t-\alpha)\sin\omega\alpha + b(t-\alpha)\cos\omega\alpha\right], \tag{4a}$$

$$\dot{b} = \frac{a}{2\omega}\left[\omega^2 - \omega_0^2 - \frac{3}{4}\beta(a^2+b^2)\right] - \frac{\mathrm{d}b}{2} + \frac{f}{2\omega} - \frac{\gamma}{2\omega}\left[a(t-\alpha)\cos\omega\alpha - b(t-\alpha)\sin\omega\alpha\right]. \tag{4b}$$

Introducing the transformation

$$a(t) = A(t)\cos\theta(t), \qquad b(t) = A(t)\sin\theta(t) \tag{5}$$

with $A^2 = a^2 + b^2$, eqs (4) become

$$\dot{A} = -\frac{\mathrm{d}A}{2} + \frac{f}{2\omega}\sin\theta + \frac{\gamma A(t-\alpha)}{2\omega}\left[\sin\omega\alpha\cos(\theta - \theta(t-\alpha))\right.$$
$$\left. - \cos\omega\alpha\sin(\theta - \theta(t-\alpha))\right], \tag{6a}$$

$$A\dot{\theta} = \frac{A}{2\omega}\left[\omega^2 - \omega_0^2 - \frac{3}{4}\beta A^2\right] + \frac{f}{2\omega}\cos\theta$$
$$- \frac{\gamma A(t-\alpha)}{2\omega}\left[\sin\omega\alpha\sin(\theta - \theta(t-\alpha))\right.$$
$$\left. + \cos\omega\alpha\cos(\theta - \theta(t-\alpha))\right]. \tag{6b}$$

In the long time limit, after transient motion, the solution (2) is periodic with period-$2\pi/\omega$ provided $a(t)$ and $b(t)$ become constants as $t \to \infty$. The limiting values of a and b are related to the equilibrium points of eqs (6). To determine the equilibrium points of (6) we set $\dot{A} = \dot{\theta} = 0$, $A(t-\alpha) = A(t) = A^*$, $\theta(t-\alpha) = \theta(t) = \theta^*$ and drop * in A and θ for simplicity. We obtain

$$\mathrm{d}A\omega - \gamma A\sin\omega\alpha = f\sin\theta \tag{7a}$$

and

$$A\left[\omega_0^2 - \omega^2 + \frac{3}{4}\beta A^2\right] + \gamma A\cos\omega\alpha = f\cos\theta. \tag{7b}$$

From eqs (7) we get

$$A^2\left[\left(\omega_0^2 - \omega^2 + \frac{3}{4}\beta A^2 + \gamma\cos\omega\alpha\right)^2 + (\mathrm{d}\omega - \gamma\sin\omega\alpha)^2\right] - f^2 = 0. \tag{8}$$

An interesting result is that in eq. (8) the time-delay parameter α appears as arguments of sinusoidal functions. If $A(\alpha_0)$ with $0 < \alpha_0 < 2\pi/\omega$ is a solution of eq. (8), then it is also the solution for $\alpha_n = \alpha_0 + n2\pi/\omega$, $n = 1, 2, \ldots$. That is, the response amplitude profile is periodic on α with period $2\pi/\omega$. There is no periodic term in (8) for $\gamma = 0$.

2.2 *Response amplitude A vs. the control parameters ω, γ and α*

Now, we analyse the variation of the response amplitude with the parameters ω, γ and α. We fix the values of the parameters as $d = 0.1$, $f = 0.05$, $\omega_0^2 = 1$ and $\beta = 2$. First, we vary the control parameter ω for fixed values of γ and α. Figure 1 shows the theoretical response amplitude curve (calculated from eq. (8)) for a range of fixed values of α for

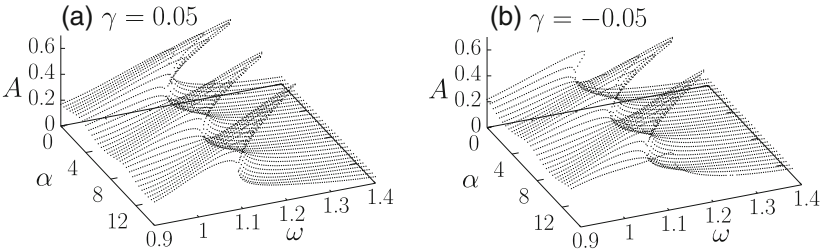

Figure 1. Plot of the amplitude A of the period-T solution of the system (1) with fixed time-delayed feedback ($x(t-\alpha)$) as a function of ω for several fixed values of α in the interval [0, 12] for $\gamma = 0.05$ and -0.05. The values of the other parameters are $d = 0.1$, $f = 0.05$, $\omega_0^2 = 1$ and $\beta = 2$.

$\gamma = 0.05$ and -0.05. The effect of positive and negative feedbacks can be clearly seen. The frequency–response curve varies periodically with respect to the control parameter α. In order to compare the theoretical response amplitude A with the numerically calculated A the equation of motion (1) is integrated using Euler method with integration step size 0.001.

In figure 2a we plot A vs. ω for $\gamma = 0.05$ and $\alpha = 1.5$ and 4.5. The result for $\gamma = 0$ is also shown. Stable and unstable parts of the response amplitude curve are represented by continuous and dashed lines respectively. The numerically calculated values of A are marked by symbols. We notice very good agreement between theoretical prediction and numerical simulation. In the absence of time-delayed feedback ($\gamma = 0$), the theoretical response amplitude is single-valued for $\omega < 1.12$ and $\omega > 1.14$. For $\omega \in [1.12, 1.14]$

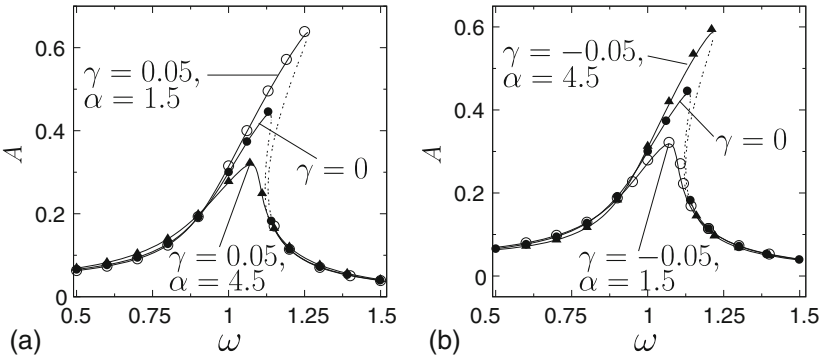

Figure 2. Amplitude A of the period-T solution of the system (1) with fixed time-delayed feedback vs. the angular frequency ω for four sets of values of γ and α. The amplitude–frequency response in the absence of feedback ($\gamma = 0$) is also depicted. Continuous and dashed lines stand for theoretically predicted stable and unstable branches respectively while the symbols stand for numerically computed values of A.

two stable period-T orbits coexist. In the numerical simulation, the two stable periodic orbits coexist for $\omega \in [1.13, 1.14]$. When the time-delayed feedback is applied, then for $\gamma = 0.05$ the interval of ω where multiple branches of response amplitude occurs initially increases with increase in α and then decreases. In figure 2a, for $\alpha = 1.5$, we notice an increase in the maximum value of A and the width of multiple branch of the response curve. In the numerical simulation, when ω increases from a small value the value of A increases and reaches a maximum value at $\omega = 1.25$. Further increase of ω results in a sudden jump to a lower value of A. When we decrease the value of ω from the value, say, 1.5, amplitude jump does not occur at $\omega = 1.25$ but it occurs at $\omega = 1.15$. The amplitude jumps from the lower branch to the upper branch. Moreover, the system exhibits hysteresis phenomenon when the parameter ω varies in the forward and backward directions. The portion of the response amplitude curve represented by dashed line cannot be realized in the numerical simulation and is an unstable branch.

The system (1) with time-delayed feedback admits two period-T solutions for a range of values of ω. For $\alpha = 1.5$ the theory predicts this interval of ω as [1.15, 1.26] while in the numerical simulation this interval of ω is [1.15, 1.25]. For a certain range of values of α, the hysteresis phenomenon is suppressed. An example is shown in figure 2a for $\gamma = 0.05$, $\alpha = 4.5$. The reverse effect occurs for $\gamma = -0.05$. In figure 2b, for $\gamma = -0.05$ and $\alpha = 4.5$, the response curve has a multivalued branch while it is absent for $\alpha = 1.5$. The widths (the interval of ω) of the hysteresis loop predicted in the theory and numerical experiments for $\gamma = -0.05$, $\alpha = 4.5$ are [1.125, 1.216] and [1.126, 1.215] respectively. Hysteresis loop can be enhanced or suppressed by appropriate time-delayed feedback.

One of the interesting results shown in figures 1 and 2 is the amplification of the amplitude A for both positive and negative values of the feedback strength γ. This feature has practical applications in many systems including nonlinear circuits, lasers and population growth. When the implementation of a particular type of feedback is not advantageous, then one can choose the other form of the feedback. For instance, in nonlinear circuits, particularly in amplifiers, the positive (regenerative) feedback gives large gain factor but with less stable and more distorted output. In contrast to this, in the case of negative (degenerate) feedback the gain factor will be relatively lower, but, the output will become

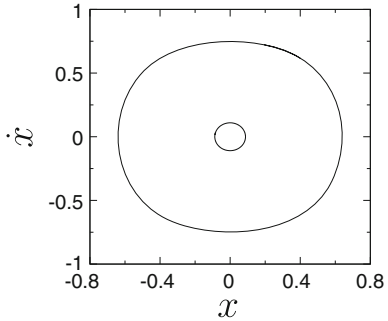

Figure 3. Phase portrait of the two coexisting periodic orbits of the system (1) with fixed time-delayed feedback with $\gamma = 0.05$, $\alpha = 1.5$ and $\omega = 1.25$.

relatively more stable with less distortion. When it is desired to have a more stable and less distorted output signal, one may prefer negative feedback.

Figure 3 shows the two coexisting period-T orbits of the system (1) for $\gamma = 0.05$, $\alpha = 1.5$ and $\omega = 1.25$. The amplitude of the inner orbit is much smaller than the other orbit. These two coexisting orbits occur in the absence of time-delayed feedback also. However, the interval of ω over which they coexist vary with the parameters γ and α. Time-delayed feedback can create an additional periodic orbit which otherwise does not exist. For example, when $f = 0.03$, $\gamma = 0.05$ and $\alpha = 1.5$ both large-amplitude and small-amplitude orbits coexist for $\omega \in [1.092, 1, 1465]$. In the absence of time-delayed feedback only small-amplitude orbit is present in this interval of ω. The presence of more than one periodic orbits with the same period can be identified from eq. (8) without explicitly calculating A. Introducing the change of variable $A' = A^2 - (s_2/3)$ eq. (8) becomes

$$A'^3 - qA' - r = 0, \tag{9}$$

where

$$q = \frac{1}{3}s_2^2 - s_1, \qquad r_1 = -\frac{2}{27}s_2^3 + \frac{1}{3}s_2 s_1 - s_0, \tag{10a}$$

with

$$s_0 = -\frac{f^2}{(3\beta/4)^2}, \quad s_1 = \frac{\left(\omega_0^2 - \omega^2 + \gamma\cos\omega\alpha\right)^2 + (\mathrm{d}\omega - \gamma\cos\alpha\omega)^2}{(3\beta/4)^2}, \tag{10b}$$

$$s_2 = \frac{2\left(\omega_0^2 - \omega^2 + \gamma\cos\omega\alpha\right)}{(3\beta/4)^2}. \tag{10c}$$

The cubic eq. (9) admits three real roots for

$$27r^2 < 4q^3, \quad q \neq 0 \tag{11}$$

and otherwise only one real root [31]. Using the above condition we can identify the regions in a parameter space, for example in (γ,α) parameter space, where more than one periodic orbit of the same period occur without calculating A.

For a range of fixed values of α, we varied ω and calculated its value at which the response amplitude A of the outer and inner orbits becomes maximum (denoted as $A_{\max}$) from the theoretical expression, eq. (8), and also by numerically solving system (1). The result is presented in figure 4 for $\gamma = 0.05$ and -0.05. Both $\omega_{\max}$ and $A_{\max}$ vary in a sinusoidal manner with the delay parameter α. The difference in the effect of $\gamma < 0$ and $\gamma > 0$ can be clearly seen in figure 4. In this figure we note that for a range of values of α, the inner orbit is not present.

Next, we vary the delay parameter α for fixed values of ω. An interesting observation from the theoretical equation for A given by eq. (8) is that it has a periodic dependence on α with period-T which is the period of the assumed periodic solution. Therefore, in figure 5 we plotted the dependence of A on α for $\alpha < 2\pi/\omega$ for a few fixed values of ω. For both $\gamma = 0.05$ and -0.05 and for $\omega < 1.092$ and $\omega > 1.275$, the amplitude A is single-valued when α is varied. Multiple branches of A are found for $\omega \in [1.092, 1.275]$. Figure 6a shows multiple branches of A and the path followed in the numerical simulation

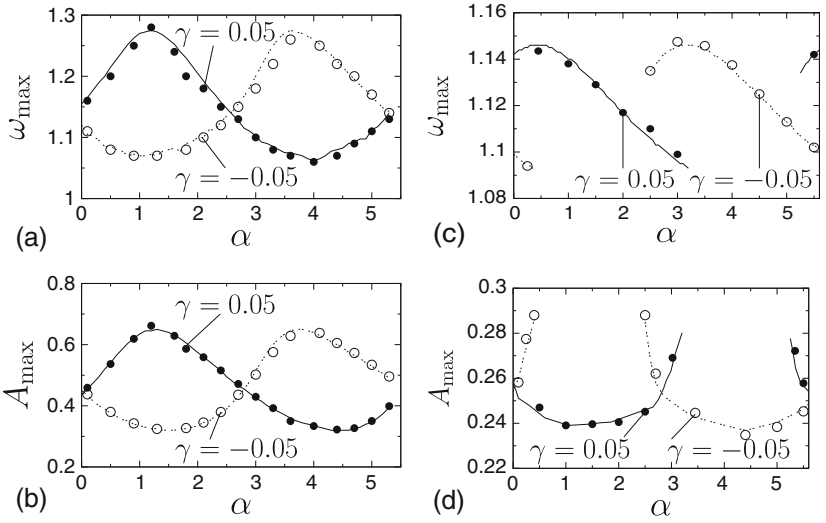

Figure 4. Variation of (**a**) $\omega_{\max}$, at which the response amplitude A of the large orbit (outer orbit is shown in figure 3) becomes maximum and (**b**) $A_{\max}$ of the large orbit with the time-delay parameter α for two fixed values of γ of the fixed time-delayed feedback. The plots (**c**) and (**d**) are for the small-amplitude orbit (inner orbit is shown in figure 3). Theoretically and numerically calculated values of $\omega_{\max}$ and $A_{\max}$ are represented by lines and symbols respectively.

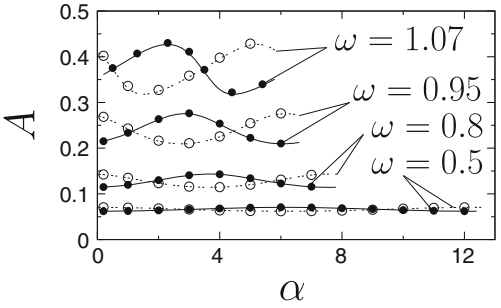

Figure 5. Variation of the response amplitude A with the control parameter α for four fixed values of ω of the system (1) with fixed time-delayed feedback. Continuous and dashed lines represent the theoretically predicted values of A for $\gamma = 0.05$ and -0.05 respectively. The symbols mark the numerically computed value of A. The response curve is single-valued. For each fixed value of ω the response amplitude is shown over $\alpha \in [0, 2\pi/\omega]$.

when α is varied in the forward and reverse directions for $\omega = 1.13$ and $\gamma = 0.05$. For $\omega = 1.13$ the multiple branches of A occur for

$$\alpha \in [1.53 + n2\pi/\omega,\ 2.74 + n2\pi/\omega], \quad n = 0, 1, \ldots. \tag{12}$$

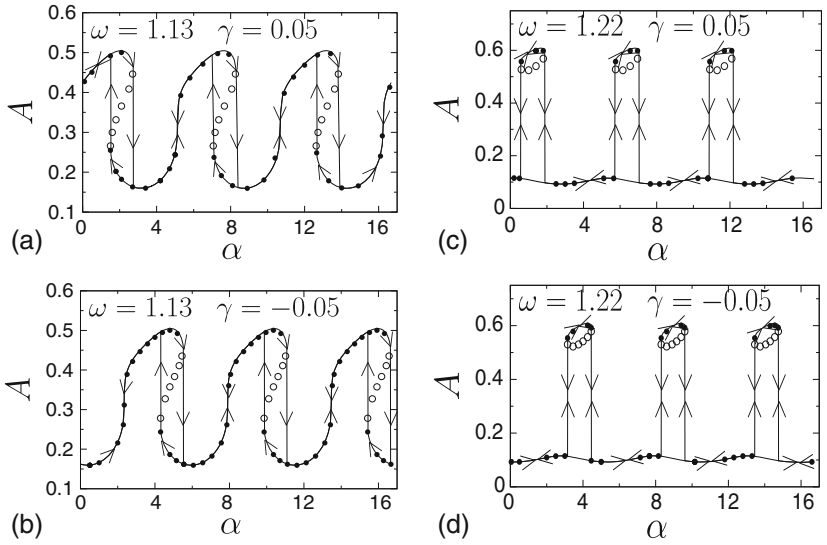

Figure 6. Response amplitude vs. the delay parameter α for two sets of values of ω and γ. In (**a**) and (**b**) where $\omega = 1.13$ different paths are followed when α is increased from 0 and decreased from a large value. In (**c**) and (**d**) where $\omega = 1.22$, A follows the same path when α is varied in the forward and backward directions. Continuous lines denote the numerical simulation. Filled and open circles represent the theoretical A in the stable and unstable branches respectively of the response curve. A is periodic with period $2\pi/\omega$.

When α is increased from a lower value, jumps from a higher value of A to a lower value of A suddenly occur at $\alpha = 2.74 + n2\pi/\omega$. On the other hand, jumps occur at $\alpha = 1.53 + n2\pi/\omega$ from a lower value of A to a higher value of A when α is decreased from a higher value. In the numerical simulation, for the starting value of α, the initial condition is $x(t) = 0.5$ for $t = 0$ to α and $\dot{x}(t) = 0$. For all other values of α the solution $(x(t),\ \dot{x}(t))$ corresponding to the previous value of α is chosen as the initial condition. The two coexisting stable branches of A found for the intervals of α given by eq. (12) are smoothly connected by the unstable branch. None of these branches exist for the entire range of values of α.

Next, in figure 6c where $\omega = 1.22$ we give an example for a different situation where a stable branch (lower branch) exists over the entire range of values of α while another stable branch occurs for certain ranges of α. A consequence of this is that hysteresis cannot occur when α is either increased or decreased from a value. In the numerical simulation we observe the solution corresponding to the lower branch when the initial condition for the present value of α is chosen as the solution of the previous α. However, if the initial condition is the same for all values of α, then jump phenomenon can occur for a certain set of initial conditions. For example, suppose the initial condition is chosen as $(x(t), \dot{x}(t)) = (0.6, 0)$ for $0 \leq t \leq \alpha$ then the upper branch of A in figure 6c is realized for the values of α for which it exists. When α is increased or decreased, sudden

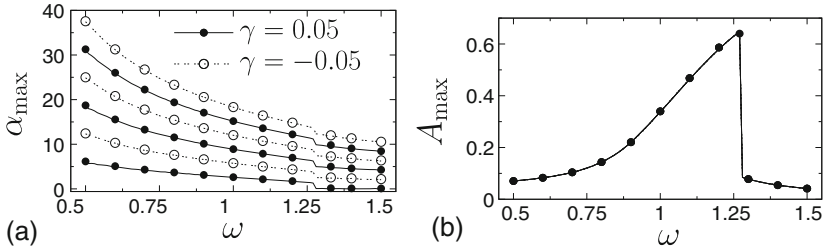

Figure 7. Dependence of (**a**) $\alpha_{\max}$ (at which the response amplitude A is maximum) and (**b**) $A_{\max}$ on the parameter ω for the system (1) with fixed time-delayed feedback. $\alpha_{\max} < 6\pi/\omega$ are alone plotted. Continuous and dashed lines represent the theoretically predicted values of $\alpha_{\max}$ for $\gamma = 0.05$ and -0.05 respectively while the symbols represent numerically computed values of $\alpha_{\max}$. In (**b**) $A_{\max}$ corresponding to $\gamma = -0.05$ and 0.05 are the same.

jumping between the upper and lower branches occurs at $\alpha = 0.57 + n2\pi/\omega$ and $1.89 + n2\pi/\omega$, $n = 0, 1, \ldots$ as depicted in figure 6c. This type of behaviour is not found in the Duffing oscillator in the absence of time-delay. That is, hysteresis can be suppressed by an appropriate time-delayed feedback. The influence of time-delayed feedback with $\gamma = -0.05$ is shown in figures 6b and 6d. These figures can be compared with figures 6a and 6c corresponding to the case $\gamma = 0.05$.

For a range of fixed values of ω we varied α and calculated its value at which the response amplitude A becomes maximum. Figures 7a and 7b present the variations of $\alpha_{\max}$ and $A_{\max}$ respectively with the angular frequency ω for $\gamma = 0.05$ and -0.05. $\alpha_{\max} < 6\pi/\omega$ alone are shown in figure 7a. $\alpha_{\max}$ is periodic with period $2\pi/\omega$. $\alpha_{\max}$ decreases with increase in ω. $A_{\max}$ increases continuously with ω and at a critical value denoted as ω_c it makes a sudden jump to a lower value due to the jump phenomenon. It is possible to find the value of ω at which $A_{\max}$ becomes a maximum without actually computing A. Suppose multiple branch of A occurs in the interval $[\omega_L, \omega_R]$. The values of ω_L and ω_R depend on the values of γ and α and is evident from figure 2. However, in figure 1 we observe that A is maximum ($A_{\max}$) at ω_R. Thus, ω_c is the value of ω_R at $\alpha = \alpha_{\max}$. The values of $\alpha_{\max}$ and ω_c, in principle, can be determined from eq. (8) or eq. (9) without calculating A. Because eq. (8) is a complicated function of A, ω and α, it is very difficult to obtain an analytical expressions for $A_{\max}$, $\alpha_{\max}$ and ω_c. $\alpha_{\max}$ and ω_c can be determined numerically from eq. (8).

3. Effect of integrative time-delayed feedback on resonance

For the system (1) with the integrative time-delayed feedback of the form $F(x(t-\alpha)) = (1/\alpha)\int_{t-\alpha}^{t} x(t')\mathrm{d}t'$, the equation for the response amplitude A is obtained as

$$A^2\left[\omega_0^2 - \omega^2 + \frac{3}{4}\beta A^2 + \frac{\gamma}{\alpha\omega}\sin\omega\alpha\right]^2 + A^2\left[\mathrm{d}\omega - \frac{\gamma}{\alpha\omega}(1-\cos\omega\alpha)\right]^2 = f^2. \tag{13}$$

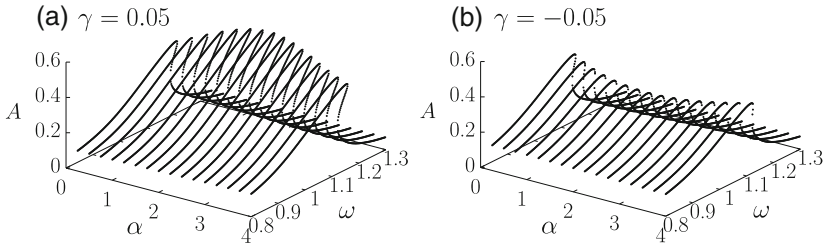

Figure 8. Theoretical frequency–response curve of the system (1) with integrative time–delayed feedback for several values of α for (**a**) $\gamma = 0.05$ and (**b**) $\gamma = -0.05$.

Equation (13) is not periodic with respect to the parameter α. However, since the assumed solution of (1) is periodic with period $2\pi/\omega$, it is reasonable to choose the value of α in $F(x(t-\alpha)) = (1/\alpha)\int_{t-\alpha}^{t} x(t')\mathrm{d}t'$ as $\alpha = \alpha \mod(2\pi/\omega)$. In this case eq. (13) is periodic on α with period $2\pi/\omega$. Therefore, in the following we restrict our analysis for $0 < \alpha < 2\pi/\omega$.

In figure 8 we plot the frequency–response curve for a range of fixed values of α for $\gamma = 0.05$ and -0.05. We note that for $\gamma = 0$, $\omega_{\max} = 1.14$ with $A_{\max} = 0.44$. In figure 8a we find that for $\gamma = 0.05$, $\omega_{\max}$ is always greater than that for $\gamma = 0$ and further $A_{\max}$ is also greater than that for $\gamma = 0$. The response is always enhanced in the positive feedback. In contrast to this for $\gamma = -0.05$, the negative feedback, both $\omega_{\max}$ and $A_{\max}$ are less than those for $\gamma = 0$. That is, response amplitude is reduced by the negative feedback. We note that in the case of nonintegrative time-delayed feedback considered in eq. (1), $A_{\max}$ varies sinusoidally about $A_{\max}(\gamma = 0)$ for both positive and negative feedbacks. Figure 9 shows ω vs. A for $\gamma = \pm 0.05$ and $\alpha = 2$ together with the result for $\gamma = 0$. We notice $A_{\max}(\gamma = 0.05) > A_{\max}(\gamma = 0)$ while $A_{\max}(\gamma = -0.05) < A_{\max}(\gamma = 0)$.

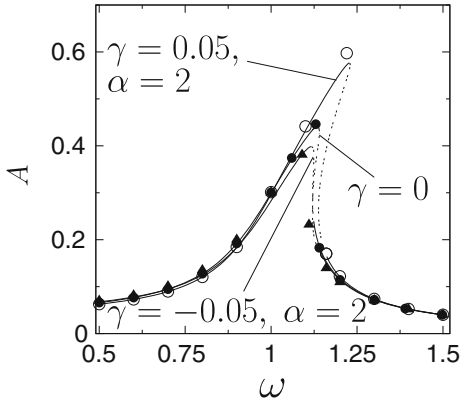

Figure 9. Frequency–response of the curve of the system (9) with integrative time-delayed feedback for two sets of values of the delay parameters γ and α. The case of $\gamma = 0$ is also shown. The continuous and dashed lines represent theoretically predicted stable and unstable branches of response amplitudes respectively. Symbols represent numerically calculated values of A at selected values of ω.

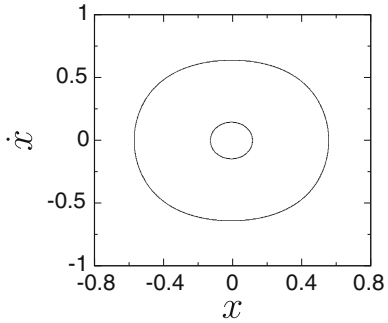

Figure 10. Phase portrait of the two coexisting periodic orbits of the system (1) with integrative time-delayed feedback for $\omega = 1.2$, $\alpha = 2$ and $\gamma = 0.05$.

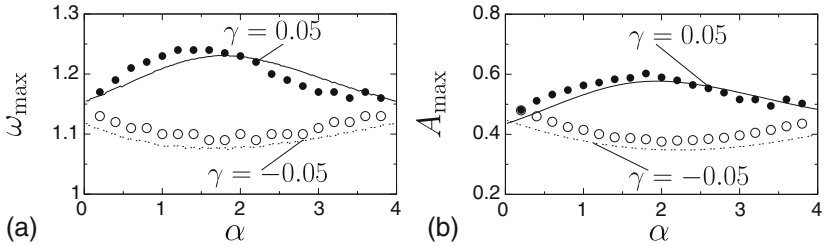

Figure 11. Variation of theoretical (represented by lines) and numerical (represented by symbols) (**a**) $\omega_{\max}$ and (**b**) $A_{\max}$ with the time-delay parameter α for $\gamma = 0.05$ and -0.05 of the system (1) with integrative time-delayed feedback.

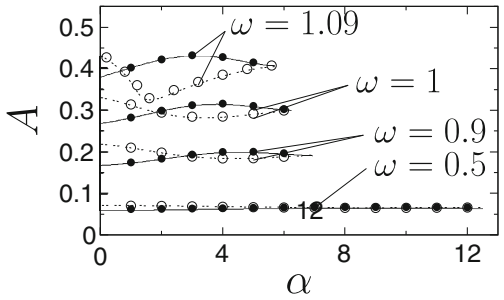

Figure 12. Response amplitude A vs. the time-delay parameter α for the system (1) with integrative time-delayed feedback. Continuous and dashed lines are theoretically calculated values of A for $\gamma = 0.05$ and -0.05 respectively. The symbols represent numerically calculated values of A. (For each fixed value of ω, A is shown only for $\alpha < 2\pi/\omega$. The response amplitude A is a periodic function of α with period $2\pi/\omega$).

Figure 10 shows the two coexisting periodic orbits for $\omega = 1.2$, $\alpha = 2$ and $\gamma = 0.05$. Figure 11 presents the variation of $\omega_{\max}$ and $A_{\max}$ with α for $\gamma = 0.05$ and -0.05. An interesting observation is that for $\gamma = 0.05$, $\omega_{\max}$ and $A_{\max}$ for $\alpha > 0$ are always greater than the respective values for $\gamma = 0$ while for $\gamma = -0.05$ they are always lower than

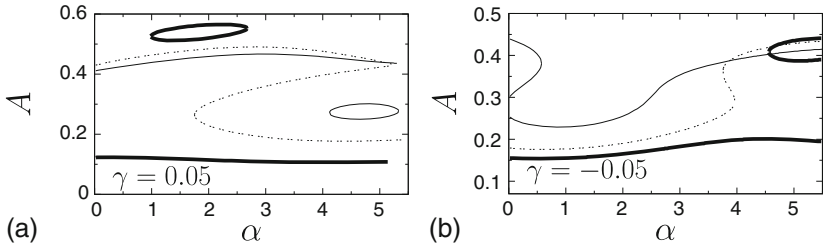

Figure 13. Theoretical response amplitude curve of the system (1) with integrative time-delayed feedback for (**a**) $\gamma = 0.05$ and (**b**) $\gamma = -0.05$. In (**a**) the values of ω for continuous, dashed and thick lines are 1.12, 1.14 and 1.21 respectively. In (**b**) the values of ω for continuous, dashed and thick lines are 1.1, 1.12 and 1.135 respectively. In all the cases the middle branch is unstable while the other two branches are stable.

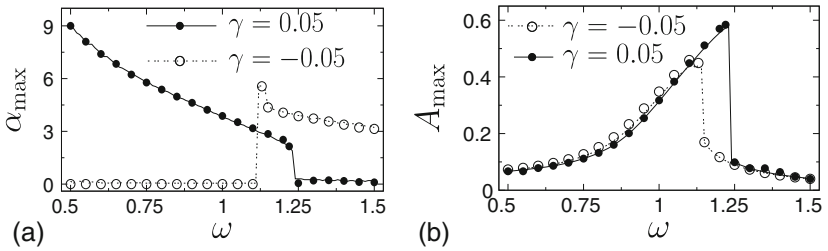

Figure 14. $\alpha_{\max}$ and $A_{\max}$ vs. the angular frequency ω of the system (1) with integrative time-delayed feedback. Theoretical and numerical values of $\alpha_{\max}$ and $A_{\max}$ are represented by lines and symbols respectively.

the respective values for $\gamma = 0$. For $\gamma = 0.05$, for each fixed value of ω in the interval [1.119, 1.231], multiple branches of A occur for a range of values of α when α is varied. For $\gamma = -0.05$ this happens for $\omega \in [1.093, 1.14]$. Figure 12 shows examples for single-valuedness of A. In this figure, for each fixed value of ω, the response amplitude A is shown only for $\alpha < 2\pi/\omega$. A is a periodic function of α with period $2\pi/\omega$. Figure 13 presents examples for multiple branches of A for both $\gamma = 0.05$ and -0.05. Figure 14 shows the variation of $\omega_{\max}$ and $A_{\max}$ with ω.

4. Conclusions

In the present work we studied the nonlinear resonance in the Duffing oscillator with fixed and integrative time-delayed feedbacks. Applying a theoretical approach we obtained the evolution equation for the amplitude of the assumed periodic solution. The frequency–response profile is found to be periodic with respect to the delay-time parameter α with period $2\pi/\omega$. The values of $\omega_{\max}$ and $A_{\max}$ are found to vary sinusoidally about $\omega_{\max}(\gamma = 0)$ and $A_{\max}(\gamma = 0)$ respectively. For a range of fixed values of α we noticed $A_{\max}(\gamma, \alpha) > A_{\max}(\gamma = 0)$. That is, response of the system is enhanced by the time-delayed feedback. In the case of fixed time-delayed feedback, the enhancement of A is realized for both positive ($\gamma > 0$) and negative ($\gamma < 0$) feedback. In contrast to this, when

the feedback is integrative, the enhancement of A occurs for $\gamma > 0$ while for $\gamma < 0$ the maximum value of A is always lower than $A_{\max}(\gamma = 0)$. For both types of time-delayed feedbacks, we have illustrated the presence of multiple branches of response amplitude curve with and without hysteresis. Jump phenomenon without hysteresis is not found in Duffing oscillator without time-delayed feedback.

Acknowledgements

The authors are thankful to the referee for the useful suggestions which improved the presentation of the present paper.

References

[1] J Chiasson and J J Loiseau, *Applications of time-delay systems* (Springer, Berlin, 2007)
[2] M Lakshmanan and D V Senthilkumar, *Dynamics of nonlinear time-delay systems* (Springer, Berlin, 2010)
[3] F M Atay, *Complex time-delay systems: Theory and applications* (Springer, Berlin, 2010)
[4] K Pyragas, *Phys. Lett.* **A170**, 421 (1992)
[5] A Prasad, J Kurths, S K Dana and R Ramaswamy, *Phys. Rev.* **E74**, 035204(R) (2006)
[6] D V Ramana Reddy, A Sen and G L Johnston, *Phys. Rev. Lett.* **80**, 5109 (1998)
[7] D V Senthilkumar and M Lakshmanan, *Int. J. Bifurcation & Chaos: Appl. Sci. Eng.* **15**, 2895 (2005)
[8] J T Sun, Y Zhang and Y H Wang, *Chin. Phys. Lett.* **25**, 2389 (2008)
[9] X Gu, S Zhu and D Wu, *Eur. Phys. J.* **D42**, 461 (2007)
[10] Y Jin and H Hu, *Physica* **A382**, 423 (2007)
[11] D Wu and S Q Zhu, *Phys. Lett.* **A363**, 202 (2007)
[12] B Kelleher, C Bonatta, P Skoda, S P Hegarty and G Huyet, *Phys. Rev.* **E81**, 036204 (2010)
[13] F Castro, A D Sanchez and H S Wio, *Phys. Rev. Lett.* **75**, 1691 (1995)
[14] Z L Jia, *Int. J. Theor. Phys.* **48**, 226 (2009)
[15] G Orosz, J Moehlis and F Bullo, *Phys. Rev.* **E81**, 025204(R) (2010)
[16] J H Yang and X B Liu, *J. Phys. A: Math. Theor.* **43**, 122001 (2010)
[17] J H Yang and X B Liu, *Chaos* **20**, 033124 (2010)
[18] C Jeevarathinam, S Rajasekar and M A F Sanjuan, *Phys. Rev.* **E83**, 066205 (2011)
[19] E M Shahverdiev and K A Shore, *Phys. Rev.* **E77**, 057201 (2008)
[20] K Hicke, O D'Huys, V Flunkert, E Scholl, J Danckaert and I Gischer, *Phys. Rev.* **E83**, 056211 (2011)
[21] T Kalmar-Nagy, G Stepan and F C Moon, *Nonlin. Dyn.* **26**, 121 (2001)
[22] B W Knight, *J. Gen. Physiol.* **59**, 734 (1972)
[23] S Ruan and G S K Wolkowicz, *J. Math. Anal. Appl.* **204**, 786 (1996)
[24] P Bak, C Tang and K Wisenfeld, *Phys. Rev.* **A38**, 364 (1998)
[25] G Golomb and G B Ermentrout, *Netw. Comput. Neural Syst.* **11**, 221 (2000)
[26] H Haken, *Euro. Phys. J.* **B18**, 545 (2000)
[27] G Saxena, A Prasad and R Ramaswamy, *Phys. Rev.* **E82**, 017201 (2010)
[28] J Li and L Zeng, *J. Phys. A: Math. Theor.* **43**, 495002 (2010)
[29] L Gammaitoni, P Hanggi, P Jung and F Marchesoni, *Rev. Mod. Phys.* **70**, 223 (1998)
[30] P S Landa and P V E McClintock, *J. Phys. A: Math. Gen.* **33**, L433 (2000)
[31] L A Pipes and L R Harvill, *Applied mathematics for engineers and physicists* (McGraw-Hill, New York, 1970)